Arab J Sci Eng (2014) 39:5677–5689
DOI 10.1007/s13369-014-1138-z

RESEARCH ARTICLE - EARTH SCIENCES

Evaluation of Temperature and Mixing Process of Water in Deep and Shallow Aquifers in the Southwestern Tunisia: Case of Djerid Region

Fatma Ben Brahim · Jalila Makni · Salem Bouri · Hamed Ben Dhia

Received: 13 April 2013 / Accepted: 31 October 2013 / Published online: 29 April 2014

Abstract This study addresses the hydrogeochemistry of thermal and cold waters circulating in the mineralised area of the Djerid basin (South-western of Tunisia) that aimed basically at understanding the mixing processes influencing their chemical compositions. Temperature intervals are 38–75 and 24.5–26.8 °C for thermal water and cold water, respectively. Two distinct hydrogeological systems supply water either for irrigation or for drinking; they are: (1) the Continental Intercalaire geothermal aquifer (CI), and (2) the Complex Terminal aquifer (CT). Geological, geophysical, hydrogeological, hydrochemical methods are applied to reliably analyze and understand the operating model of the aquifer systems, to determine the hydrogeological, the geochemical behaviours, and the possible inter-aquifers water transfer in south western of Tunisia. The reservoir temperature is estimated to be between 60 and 104 °C according to calculations using silica geothermometers and computation of saturation indexes for different solid phases. Based on chemical and thermal data, it is hypothesized that: (1) mixing rate, which occurs between the ascending deep geothermal water and shallow cold water, is estimated from the enthalpy and chloride methods to be about 65 and 73 % respectively, (2) Mixing models can explain the temperature of the geothermal fluid component.

Keywords Aquifer · Temperature · Hydrochemistry · Mixing · Fraction · Djerid region

الخلاصة

تم في هذه الورقة العلمية دراسة بعض الخصائص الفيزيائية والكيميائية للمياه الجوفية الحارة والباردة الموجودة في منطقة الجريد (جنوب غرب تونس)، وهي تهدف في الأساس إلى فهم عمليات المزج وكيفية تأثيرها في التركيبة الكيميائية للمياه.

تتراوح درجات الحرارة بين 38-75 درجة مئوية بالنسبة للمياه الحارة، وبين 24.5 – 26.8 درجة مئوية بالنسبة للمياه الباردة. وتتدفق الموارد المائية من خزانين يتميزان بتوفير المياه الصالحة سواء أكان للري أم للشرب وهما: (1) طبقة المياه الجوفية الحارة (CI) ، و (2) مجمع طبقة المياه الجوفية الطرفية (CT). واعتمادا على النتائج الأولية للأبحاث الجيولوجية والجيوفيزيائية والهيدروجيولوجية ودراسة بعض الخصائص الفيزيائية والكيميائية للمياه تمكنا من فهم النموذج التشغيلي لطبقات المياه الجوفية وتحديد السلوكيات الهيدروجيولوجية والجيوكيميائية ، وكيفية انتقال المياه بين مختلف طبقات المياه الجوفية في الجنوب الغربي التونسي.

وقد تم ـ إضافة إلى ذلك ـ تقدير درجة حرارة مياه الخزان الحار ما بين 60 و 104 درجة مئوية وفقا لحسابات استخدام جيوترمومتر السيليكا وحساب مؤشرات التشبع للمراحل الصلبة المختلفة. واستنادا إلى مختلف البيانات الجيوحرارية تم تقدير نسبة معدل الاختلاط الذي يحدث بين المياه العميقة الحارة الصاعدة والمياه البارد ة (حوالي 65 ٪ باستخدام نظرية أسلوب المحتوى الحراري، وحوالي 73 ٪ اعتمادا على طريقة الكلوريدات).

1 Introduction

Composition of thermal well waters is sometimes the result of fluid mixing in the reservoir and/or in the well [1]. In such cases, it is impossible to obtain numerically a unique solution to the problem of origin, in terms of chemical characteristics, estimated temperature in depth, etc., without assuming that all of the given chemical components are of the same origin

The mixing between shallow and thermal groundwater and gain or loss of steam, may modify the chemistry of the ascending fluids and lead to erroneous interpretations [2,3]. Several workers have proposed a method that uses the chemical composition of the water to find the ratio of the fraction

F. Ben Brahim (✉) · J. Makni · S. Bouri · H. Ben Dhia
Water, Energy and Environment Laboratory (LR3E),
National School of the Engineers, B.p.w.3038 Sfax, Tunisia
e-mail: bfatma27@yahoo.fr

mixing and the origin temperature (e.g. [2,4]). In addition, the chemistry of thermal waters has attracted the attention of numerous studies, in particular investigations of the influence of water–rock interactions and the large diversity of the ionic composition of fluids that are found in geothermal systems (e.g. [5–14]).

Tunisia has an important geothermal potential that is well-known since the Roman period. Tunisia is known with more than 90 thermal manifestations including 50 thermal springs.

Southwestern Tunisia constitutes an important hydrothermal basin. This region was the subject of different hydrogeothermic studies [15–17]. The most important aquifers hosted in Cretaceous formations are composed of sandstone (Continental Intercalaire aquifer) and limestone (Miocene and Senonian aquifers). Continental Intercalaire (CI) aquifer is characterised by thermal water, whereas Turonian and Senonian aquifers supply cold waters.

To assess hydrogeothermal resources of South-western of Tunisia, hydrogeothermal study comprising geological, hydrogeological, hydrogeochemical and geothermometric approaches have been realized. This approach is important for the determination of the different hydrogeochemical facies of thermal and cold waters, and to relate them to their original reservoirs, providing a good tool for delimiting the hydrothermal basins.

One of the major tasks in the exploration of geothermal resources is the estimation of the subsurface temperature using geochemical composition of thermal springs and the evaluation of the mixing water ratio. This paper aims to characterise thermal and cold waters in order to study the water exchange between the deep and shallow aquifer systems (Continental Intercalaire and Complex Terminal) using a hydrogeothermal approach.

2 Study Area

Djerid region is located in the South western part of Tunisia (Fig. 1) and is characterized by an arid climate with annual average precipitation of 98 mm. The maximum temperature is about 45 °C (August) and the temperature range is very high. These difficult conditions require a large amount of water to maintain humidity inside the oases systems.

The Djerid area occupies an intermediate position between El Gharsa Chott and Djerid Chott (Fig. 2), constituting the western extent of the Chotts fold belt [18], which corresponds to the most southern structures of the Atlassic domain [19–26].

The age of geological formations ranging from lower Cretaceous to Plio-Quaternary are largely outcropped in the Southwestern Tunisia (Table 1). Available data from geological and geophysical studies have provided the means to identify the main potential hydrogeological entities (Figs. 2, 3):

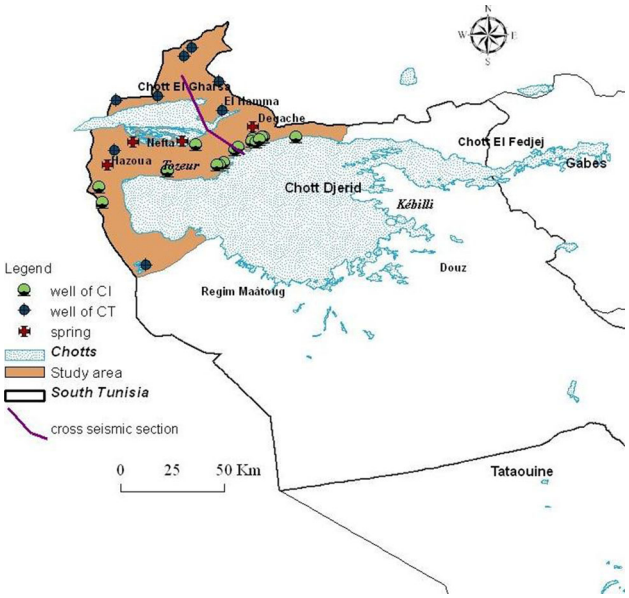

Fig. 1 Location of the study area

2.1 The Complex Terminal Aquifer (CT)

The CT is represented in the Djerid area by the Miocene–Pliocene continental sedimentary rocks of Beglia and Segui formations [27–29].

The Beglia formation (Miocene) has an average thickness of 100 m and is made up of fine to coarse sands with thin clayey intercalations. The Segui formation (Miocene–Pliocene) is essentially clayey. It is enriched in sands with its thickness decreasing towards the eastern part of the Djerid. However its maximum thickness attains 500 m in Mzaara well which is implanted in the western part (Figs. 1, 2).

2.2 The Continental Intercalaire Aquifer (CI)

The CI is defined as the set of sedimentary layers that comprise mainly continental sandstone-clay formations of the Lower Cretaceous age.

The CI has been described by Cornet [30] and Castany [31] and an account is given here only of essential aspects relevant to hydrogeological interpretation. In the Djerid region, the aquifer extends from the Gafsa–Metlaoui chain, which makes part of the Saharan Atlas, to the extreme south of the country [19]. The geological formations hosting the CI aquifer change in facies and in thickness from the Chotts area towards the Saharan platform. Changes in sedimentation within the fluvio-deltaic continental deposits produce alternating layers of detrital beds with clayey silt and gypsum intercalations [32].

In The Djerid the CI aquifer is about 180 m thick (Figs. 2, 3). It has been observed within three permeable formations (Table 1): (a) the Hauterivian–Barremian clayey sandstone

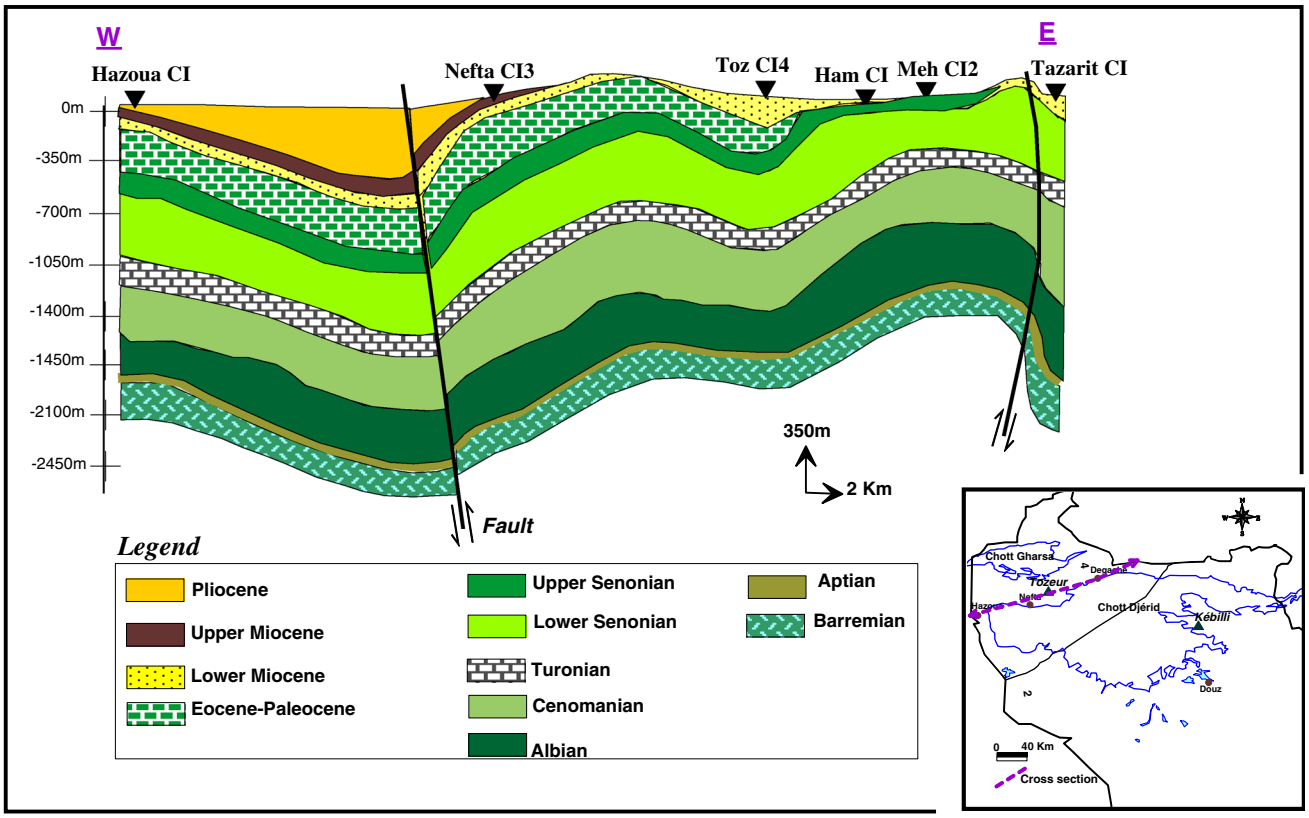

Fig. 2 Hydrogeological cross section for the Djerid region

Table 1 Hydrogeological, stratigraphic units and geological formations in the aquifer systems in the Djerid area

Hydrogeological units	Stratigraphic units	Djerid region Formation name/lithology
Plio-Quaternary (PQ)	Quaternary	Unnamed quaternary terraces/sands and clay with some gypsum
	Pliocene	Unnamed/sandy clay
Complex Terminal (CT)	Miocene	Beglia and Segui/sands and clay
	Senonian	Abiod/fissured limestone
Aquitard	Santonian–Coniacian	Aleg/sandy clay
	Turonian–Cenomanian	Zebbag/limestone and clayey dolomite
Continental Intercalaire (CI)	Aptian–Albian	Orbata/sandstone, limestone and marl
	Aptian	Sidi Aïch/sands and sandstone
	Barrem.–Aptian	Bouhedma/silt, clay and dolomite
	Hauterv–Barrem.	Boudinar/clay and sandstone
	Valanginian–Hauterv.	Sidi kralif/clay
Substratum	Jurassic	Nara/limestone, dolomite and clay

(Boudinar formation), (b) the Aptian sands and sandstone (Sidi Aïch formation), and (c) the Aptian–Albian sandstone, limestone and marl (Orbata formation). The main confined aquifer horizon is however the Sidi Aïch formation found at a depth between 1,300 and 2,200 m [33].

The hydrostratigraphic units in the Djerid basin (Fig. 3) are shown in a SSE–NNW seismic section [18]. These units consist of two main aquifer systems: namely, from the top to the bottom: the Upper Cretaceous (CT) and the Lower Cretaceous (CI) which extends over the whole basin. This section shows also the reduction of thickness of these formations and unconformities related to rejuvenation of master faults associated with Triassic evaporate risings.

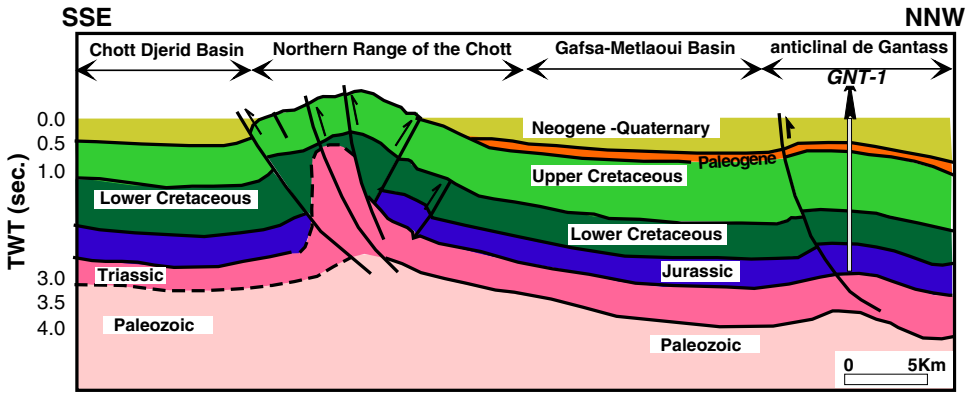

Fig. 3 Interpretation of seismic section crossing the Gantass and Northern range of the Chotts [18]

3 Materials and Methods

Several analyses such as the water temperature, pH, electrical conductivity (EC), and total alkalinity as HCO_3 were carried out on-site. All samples for chemical analyses were collected in low density polyethylene bottles and filtered in the laboratory through 0.45-μm membrane filters. Samples revealing relatively high salinity (exceeding 3 g/l) were diluted before analysis.

Each sample was collected in two new 500-ml polyethylene bottles. All sampling bottles were washed with deionised water and again with filtered sample water before filling it to capacity. For each sample, one bottle is acidified (until pH of samples reached 1) with 35 % nitric acid for cation analysis (Na^+, K^+, Ca^{2+} and Mg^{2+}), whereas the other is used for the determination of dissolved anions (Cl^-, $SO_4{}^{2-}$, $HCO_3{}^-$ and $SiO_2{}^-$). Prior to analysis in the laboratory, the samples were stored at a temperature below 4 °C. Chloride was determined by the standard titration method or the Mohr method. Bicarbonates was determined by the potentiometric method. Sulphate concentration was measured by the gravimeter method using $BaCl_2$. Sodium and potassium concentrations were determined with a flame photometer.

Calcium and magnesium ions were determined by the complexation method using ethylene diamine tetra-acetic acid bisodium salt. Total dissolved solids (TDS) were measured by evaporating a pre-filtered sample to dryness.

Twenty two samples were collected from thermal and cold wells and springs (Fig. 1). The quality of the analyses was evaluated using the ion balance (IB) and only ones with IB < 5 % were considered.

4 Results and Discussion

4.1 Hydrochemical Study

Analytical results of major ions in groundwater samples are given in Table 2. Samples collected from the CI aquifer are characterized by high temperature varying from 38 to 75 °C, low-temperature waters with 24.5 to 49 °C characterize the CT groundwater. Values of water temperature and depth of boreholes are not well correlated probably due to the large screens characterizing these deep CT and CI boreholes.

The Total dissolved solids (TDS) values in the CI groundwater range from 1.908 to 7.052 mg/l. Those of the CT aquifer vary between 1.318 and 4.392 mg/l. The Piper trilinear diagram [34] is given in Fig. 4 and it shows that the dominant cations are mainly calcium and sodium, while the dominant anions are sulphate and chloride. The sum of cations and anions shows two main groundwater types: Na–Cl and Ca–SO_4.

The Piper diagram shows that the waters from the Lower Cretaceous aquifer are situated close to the Na–Cl vertex, probably due to the leaching of evaporitic minerals. However, waters from both the wells and springs in the Djerid region are Ca–(Na)–SO_4–(Cl) mixed water type, possibly due to the presence of evaporate minerals (gypsum and/or anhydrite ($CaSO_4$)) in this two aquifers.

Furthermore, bivariate diagrams of major elements were used to separate different mechanisms that contribute to groundwater mineralization.

In particular, sodium versus chloride and calcium versus sulphate show positive correlations (Figs. 5, 6). This indicates the possible dissolution of halite in CI aquifer, gypsum and/or anhydrite-bearing rocks are relatively abundant especially in the Lower Miocene (CT) and Cretaceous (CI) aquifers.

As an attempt to distinguish the major groups of water, the correlation between sulphate and temperature (Fig. 7) reveals three groups: cold water (Miocene (CT) on majority), mixing water (between CI and CT) and thermal water (CI).

The multivariate statistical analysis is a quantitative and independent approach of groundwater classification which allows the grouping of groundwater samples and the making of correlations between chemical parameters and groundwater. Correlation coefficient is a commonly used measure to establish the relation between independent and dependent variables [35].

Table 2 Chemical composition of the Southwestern groundwaters (in milligrams per liter)

No.	Well	Aquifer	Aquifer name	pH	*T* (°C)	TDS	Ca	Mg	Na	K	HCO_3	Cl	SO_4	SiO_2
1	Rmitha	Beglia formation (Lower Miocene)	CT	7.9	25	2,855	385.8	88.1	396.3	14.71	152.5	634.2	1,183.3	
2	Tamerza SONEDE	–	CT	7.4	24.5	1,318	171	37.9	179.8	4.38	146.4	151.8	626.3	
3	Ben Guecha	–	CT	8.1	38	3,818	428.4	121.9	706.3	22.82	164.7	1,026.9	1,347.1	
4	Segdoud CT3	–	CT	7.6	39.8	2,571	296.6	78.4	400.9	23.3	140.3	696.5	935.1	18
5	Dafria CT1	–	CT	7.9	40	4,392	336	326	565	24	396	1,065	1,680	19
6	Dhafria CT 3	–	CT	8	49	3,601	500	120	460	11.7	244	1,063	1,200	
7	Htam	–	CT	7.2	37.4	2,886	306.2	85.5	480.6	10.2	106.4	760.6	1,146.2	40
8	Bir Roumi	–	CT	7.2	26.8	2,803	372.1	89.9	361.6	16.7	146.4	602.4	1,214.2	
9	Degache CI 3	Sidi Aïch formation (Barremian–Aptian)	CI	6.7	74	2,209	349.9	29.6	316.7	66.78	231.8	436.7	777.6	40
10	Hamma CI 1bis	–	CI	7.5	73	2,414	314.1	19.5	427.9	37.75	134.2	334.3	1,145.9	
11	Ceddada CI	–	CI	7.1	38	2,243	308.3	22.2	326.1	52.88	146.3	437	950.6	33
12	Mzaraa CI	-	CI	6.8	73	1,908	309.4	56.9	215.9	76.32	134.2	327	788.6	45.2
13	Hazoua CI4	–	CI	7.9	60	3,349	414	68.5	531	71.9	142	602	1,520	37
14	Nefta CI 1	–	CI	7.3	70	3,327	412	66.5	529	69.9	140	600	1,510	
15	Nefta CI 2	–	CI	7.2	72	2,695	371	43.4	374	62.9	144	320	1,380	
16	Tozeur CI1	–	CI	7.2	67	7,052	889	279	3,500	79.8	104	5,960	1,840	44
17	El Hamma CI2	–	CI	8.2	64	3,358	304	29.9	652	46.3	256	360	1,710	
18	Mahasen CI1	–	CI	6.9	69.5	2,287	355	41	277	89	179	371	975	
19	S.Sidi Abdelkader	–	CI	7	75	2,299	336	38.9	424	60	146.4	887	1,688	52
20	S.El Borma	–	CI	6.9	75	2,736	372	138.6	648.6	23.4	140.3	1,001.1	1,339.2	51
21	S.Nefta	–	CI	8	65	2,736	520	31.6	500	92.5	170.8	603.5	1,200.5	42
22	S.Rejel	–	CI	6.9	75	2,736	372	138.6	648.6	23.4	140.3	1,001.1	1,339.2	50

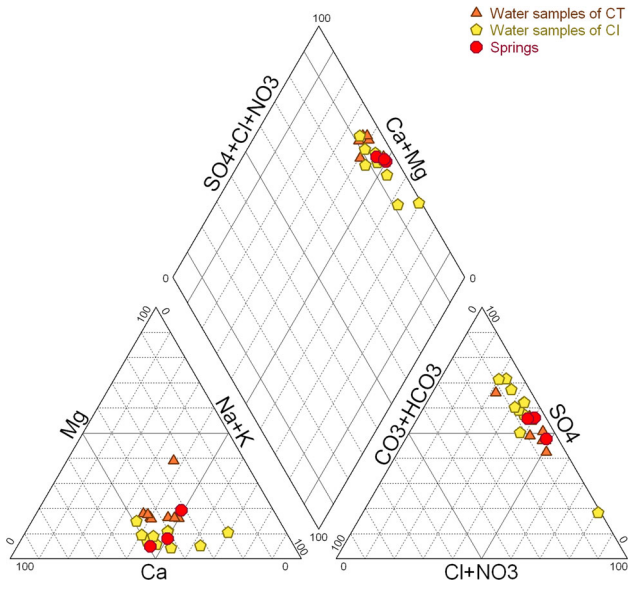

Fig. 4 Piper diagram of the groundwater

Principal component analysis (PCA) was performed on a data set of 22 samples and the eigenvalues and the percentage of the variance explained by each eigenvector is listed in Table 3. Two principal components or factors (eigenvalue) explaining 68.3 % of the variance or information contained in the original data set are retained, which are sufficient to give a good idea of the data structure.

Factor 1 (F1) explains more than 46.5 % of total variance and contains large loadings on Na^+, Cl^-, Ca^{2+}, $SO_4{}^{2-}$ and TDS. It represents the weathering of halite and evaporates minerals from the underlying formations. Factor 2 (F2) contributes to 21.8 % of the total variance and is strongly associated with K^+, $HCO_3{}^-$, *T* (°C) and pH.

The scores of variables and observations onto the two principal component axes are plotted in Fig. 8, which enables identification of several processes of water mineralization.

The contents of chloride, sodium, calcium, magnesium and sulphates are positively correlated with salinity in all waters, with correlation coefficients of 0.94, 0.93, 0.84, 0.67

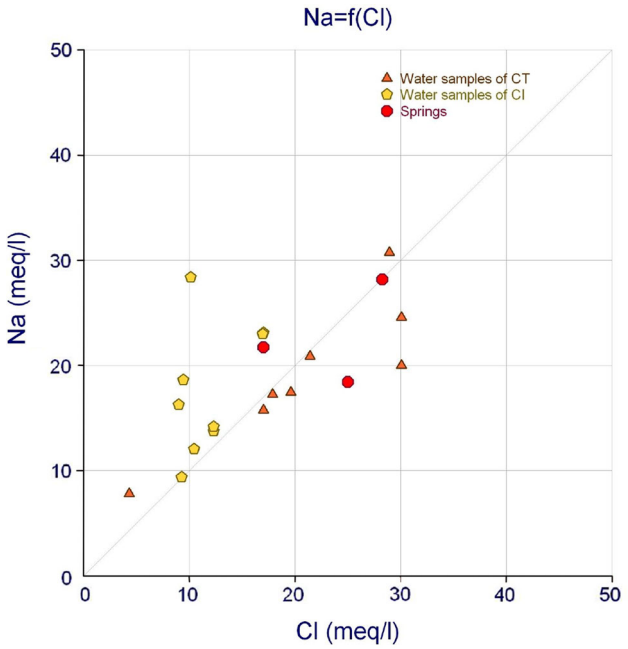

Fig. 5 Na/Cl relationship

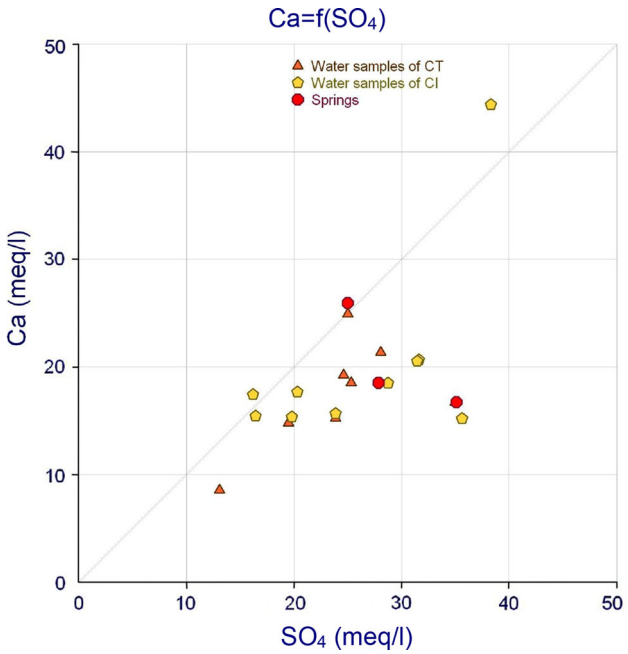

Fig. 6 Ca/SO_4 relationship

and 0.51, respectively. Sodium and chloride are correlated with a coefficient of 0.98 (Table 4).

They have a common natural origin that would be mainly the dissolution of halite (NaCl). Also, SO_4 and Ca have a correlation coefficient of 0.52, indicating that the origin is the dissolution of $CaSO_4$.

Individual representation (samples) in the first factorial plan (F1 × F2) classifies groundwater in two different groups

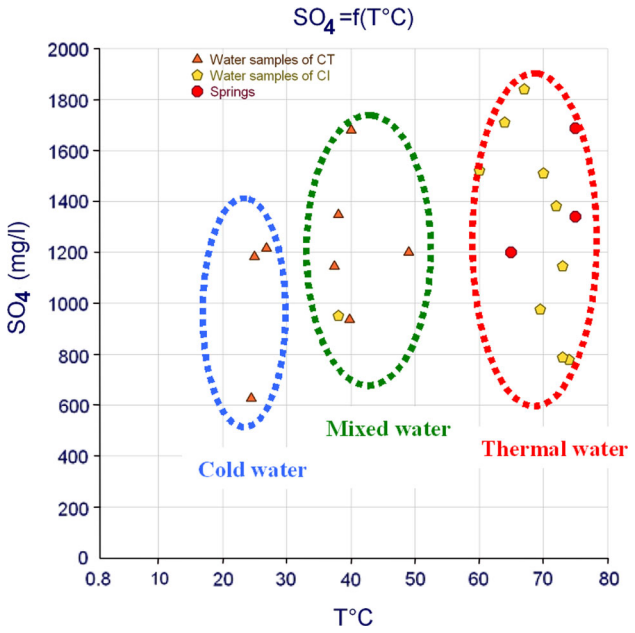

Fig. 7 Relationships between temperature and sulphate ions in the groundwater samples

(Fig. 9): i.e., (i) a group representing the trend of halite dissolution essentially for CI groundwaters and (ii) a group representing the trend of gypsum dissolution essentially for Miocene waters.

4.2 Geothermometry Approach

Dissolved chemical species are widely used to obtain information on subsurface temperatures using multiple fluid–mineral equilibrium calculations. Chemical geothermometers depend upon the water–mineral equilibrium and give the last equilibration temperature in the reservoir [36].

Several types of chemical geothermometers are described in the literature (e.g. [10,37,38]).

The correlation matrix of physical parameters (T, pH and TDS) and SiO_2 has been given in Table 5. This PCA reveal a good correlation between T and SiO_2 ($r = 0.86$). The projection of variables onto the factorial plan (F1 × F2) reveals the good correlation between the temperature and the silica content (Fig. 10). The representation of individual spaces reveals three types of water: thermal water (from the CI aquifer), cold water (From Miocene aquifer) and mixing water.

One practical and often used application of surface water geochemical analyses is the calculation of subsurface temperatures using chemical geothermometers. Several types of these geothermometers have been studied. According to Fournier [39], silica is ideal for this purpose as it is generally in excess supply (as it is the main constituent of the vast majority of minerals). He compiled various equations relating temperature with solubility with guidance as to

Table 3 The principal component analysis results

Component	Total	Eigenvalues	Cumulative variance %	% of variance	Cumulative %
1	4.653	46.528	46.528	46.528	46.528
2	2.179	21.787	68.315	21.787	68.315
3	1.304	13.036	81.351		
4	0.807	8.070	89.421		
5	0.547	5.472	94.894		
6	0.200	1.997	96.891		
7	0.161	1.606	98.497		
8	9.460E−02	0.946	99.443		
9	4.874E−02	0.487	99.930		
10	6.982E−03	6.982E−02	100.000		

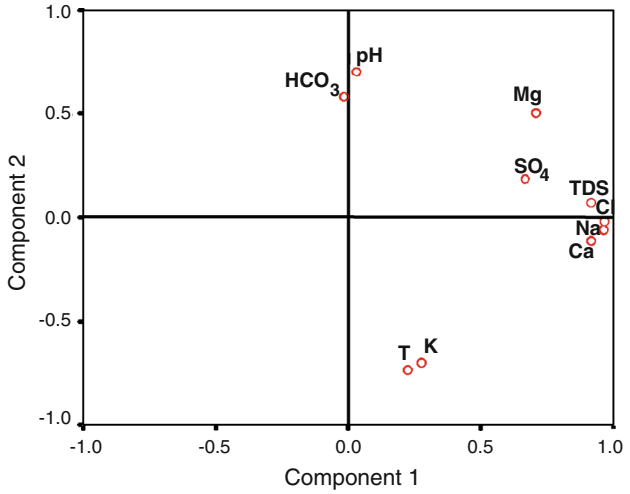

Fig. 8 Projection of variables onto the factorial plane (F1 × F2)

their usage for amorphous silica, quartz (assuming maximum steam loss and no-steam loss), cristobalite (α and β types) and chalcedony. These results seem to be reliable values.

In this study, the good correlation between SiO_2 and temperature can be a good tool to estimate the reservoir temperature of the thermal aquifer. In fact, quartz geothermometers indicate relatively adequate temperatures (Table 6). It reveals an estimated temperature at about 60 °C, for the CT aquifer, and between 60 and 104 °C for the CI aquifer, with a good correlation between the emergency temperatures and the estimated ones (Fig. 11).

4.3 Mineral Equilibrium Calculations

Modelling of the state of equilibrium at different temperatures is another approach to estimate the temperature of the thermal reservoir, especially in the presence of carbonate and evaporate host rocks [40,41].

Equilibrium between an assemblage of minerals constituting an aquifer and a groundwater depends on the temperature. Formulating a numerical model to calculate the saturation state of various likely aquifer minerals at a specified temperature, in a particular groundwater, allows gauging the degree of fluid–mineral equilibrium. By recalculating over

Table 4 Correlation matrix 1

Correlation	pH	*T*	TDS	Ca	Mg	Na	K	HCO_3	Cl	SO_4
pH	1.000									
T	−0.422	1.000								
TDS	−0.013	0.090	1.000							
Ca	0.082	0.228	0.841	1.000						
Mg	0.139	−0.133	0.666	0.517	1.000					
Na	−0.022	0.164	0.925	0.873	0.608	1.000				
K	−0.228	0.660	0.195	0.379	−0.203	0.229	1.000			
HCO_3	0.404	−0.100	0.008	−0.137	0.391	−0.174	−0.101	1.000		
Cl	−0.065	0.112	0.938	0.879	0.667	0.983	0.176	−0.155	1.000	
SO_4	0.308	0.261	0.507	0.521	0.518	0.540	0.148	0.199	0.499	1.000

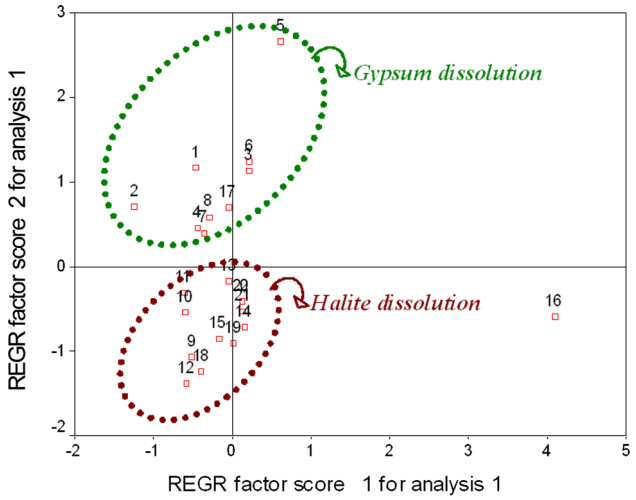

Fig. 9 Projection of samples onto the factorial plane (F1 × F2)

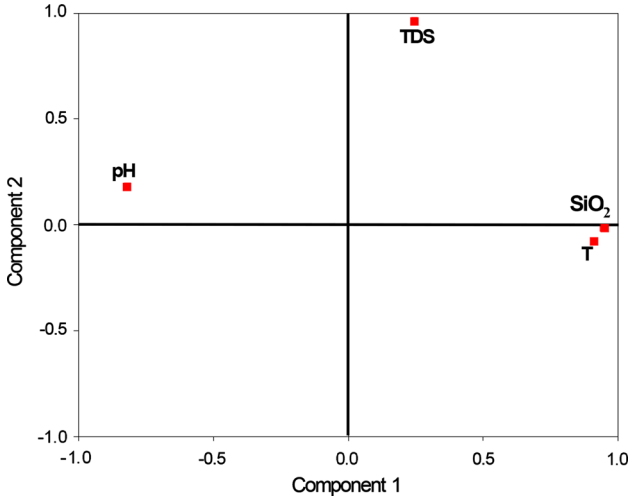

Fig. 10 Projection of variables (T, pH, TDS and SiO_2) onto the factorial plane (F1 × F2)

Table 5 Correlation matrix 2

Correlation	pH	SiO_2	T	TDS
pH	1.000			
SiO_2	−0.668	1.000		
T	−0.599	**0.857**	1.000	
TDS	−0.064	0.193	0.132	1.000

Bold shows the high value of correlation

a range of temperatures, we can deduce saturation indexes (SI $=$ $\log \mathrm{IAP}/K_T$, where IAP is the ionic activity product, and K_T is the equilibrium constant of the mineral at the discharge temperature of the sample) as a function of temperature. Theoretically, if the SI values with respect to several minerals converge to zero at or around a particular temperature, this value is considered to represent the temperature of chemical equilibrium in a geothermal reservoir [42,43].

Furthermore, many researchers worldwide [16,41,44–48] used the SI of a set of minerals in the fluid to constrain the temperature condition and to distinguish between equilibrated and non-equilibrated waters, as non-equilibrated waters show a large range of mineral saturation temperatures.

Mineral equilibrium calculations are also important to predict which minerals may precipitate during the extraction and the use of the waters. A saturation index of zero indicates a thermodynamic equilibrium between water and the solid phase of the relevant mineral. A negative (−) or positive (+) index reflects undersaturation or oversaturation, respectively.

Saturation indexes of some common minerals were calculated using the programme HYDROWIN [49].

Figure 12 depicts some changes of mineral SI, calculated with an increasing temperature for samples of the Djerid waters. Then, SI for each mineral was plotted versus temperature, and the trend curves were represented. For the Sidi Abdelkader, El Rejel and El Borma springs (water with discharge temperature = 75 °C) (Fig. 12a), the saturation indexes of the water with respect to quartz, gypsum, and magnesite tend to get closer to zero around the temperatures of 100 °C. For the Dhafria CT3 well (water of CT with discharge temperature = 49 °C) (Fig. 12b), the SI in relation to anhydrite, gypsum, quartz and chalcedony converge exactly close to zero at ∼75 °C. For the Degache CI well (water of CI with discharge temperature = 74 °C) (Fig. 12c), SI related to quartz, gypsum and magnesite converge below the zero at ∼100 °C.

These findings suggest that the thermal waters of Djerid region are partially equilibrated waters fed by geothermal fluids at different temperature between 75 and 100 °C. This can indicate the contribution of various fluids having different temperatures.

It can be noted that the silica geothermometers gives, for the Djerid thermal waters, quite different equilibrium temperatures, and thus, implying that these waters are “immature”, and not equilibrated-waters. The SI method, however, shows that thermal waters are partially equilibrated with evaporate minerals at temperatures significantly close to quartz temperatures.

4.4 Hydrodynamic Relationship

The study of the hydrodynamic relationship between CT and CI aquifers revealed the existence of an exchange between the two superposed aquifers, which are controlled by dominant sub-vertical faults affecting the southwestern Tunisia especially the Djerid basin. The direction of drainage is determined by the difference of pressure for the two aquifers. The projection of Piezometric profiles (Fig. 13) shows that throughout the study area, the water flow is upward, and the water supplies of CI groundwater overlying the CT.

Table 6 Estimated reservoir temperature (°C) by the Silica geothermometers [39] for the Djerid region water samples

Water samples	Aquifer	SiO_2	Surface temperature (°C)	QSP V	QAP V	Chalcedony	α-Cristobalite	β-Cristobalite	Amorphous silica
Segdoud CT3	CT	18	39.8	60	65	27	11	−33	−49
Dhafria CT3	CT	19	40	62	67	29	12	−31	−48
Degache CI	CI	40	74	92	94	61	42	−5	−23
Hazoua CI4	CI	37	60	88	91	57	38	−8	−26
Tozeur CI1	CI	44	65.5	96	97	66	46	−1	−19
Ceddada CI	CI	33	38	83	87	52	33	−12	−30
Mzaara CI	CI	45.2	73	97	99	67	47	0	−18
S.Sidi Abdelkader	CI	52	75	104	104	74	53	6	−12
S.Nefta	CI	42	65	94	96	63	44	−3	−21
S.El Borma	CI	51	75	103	103	73	52	6	−13
S.Rejel	CI	50	75	102	103	72	51	5	−14

QSPV quartz-no steam loss, *QAPV* quartz-maximum steam loss at 100 °C

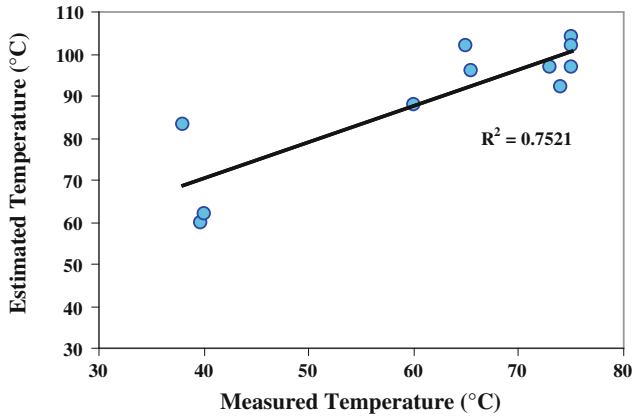

Fig. 11 Correlation between measured and estimated temperatures

4.5 Evaluation of Mixing Processes

4.5.1 Enthalpy Method

The ascending thermal waters are usually mixed with shallow cold water. Mixing processes are traced by chemical composition of the mixed waters and two end members (i.e. cold and thermal water). The temperature of the thermal water and the proportion of the thermal and cold waters in mixing can be estimated based on the chemical contents of cold and mixed water samples. To determine the two unknowns, two equations can be written and solved [50]. The first equation relates the enthalpies of the thermal water (H_h), cold water (H_C) and spring water (H_S) and the fractions of cold water, X, and of thermal water $(1 - X)$,

$$H_C(X) + H_h(1 - X) = H_S$$

The second equation relates the silica contents of thermal water (Si_h), cold water (Si_C), and spring water (Si_S):

$$Si_C(X) + Si_h(1 - X) = Si_S$$

These two equations can be solved for the two unknowns.

Here, a graphical approach suggested by Fournier and Truesdell [2] is used for determining the unknowns in the studied thermal waters [50]:

1. Table 7 lists enthalpy as a function of temperature for liquid water [2]; the fraction X_t is calculated for each temperature value as follows:

$$X_t = \frac{H_h - H_S}{H_h - H_C}$$

2. X_t is plotted against the temperatures (curve labeled enthalpy in Fig. 14).
3. A series of values of the silica contents of thermal water for the temperatures listed in Table 7 [2] is considered, and X_{Si} is calculated for each value as follows:

$$X_{Si} = \frac{Si_h - Si_S}{Si_h - Si_C}$$

X_{Si} is plotted against temperature on the same graph (curve labeled silica in Fig. 14). The point of intersection of these two curves gives the estimated temperature of the thermal water component and the fraction of the cold water.

The intersection of the two curves in Fig. 14 shows that the cold water fraction is about 0.65 and that the temperature of the thermal water is inferred to be less than 120 °C. The average contribution of cold water in the studied thermal waters is estimated to be about 65 %.

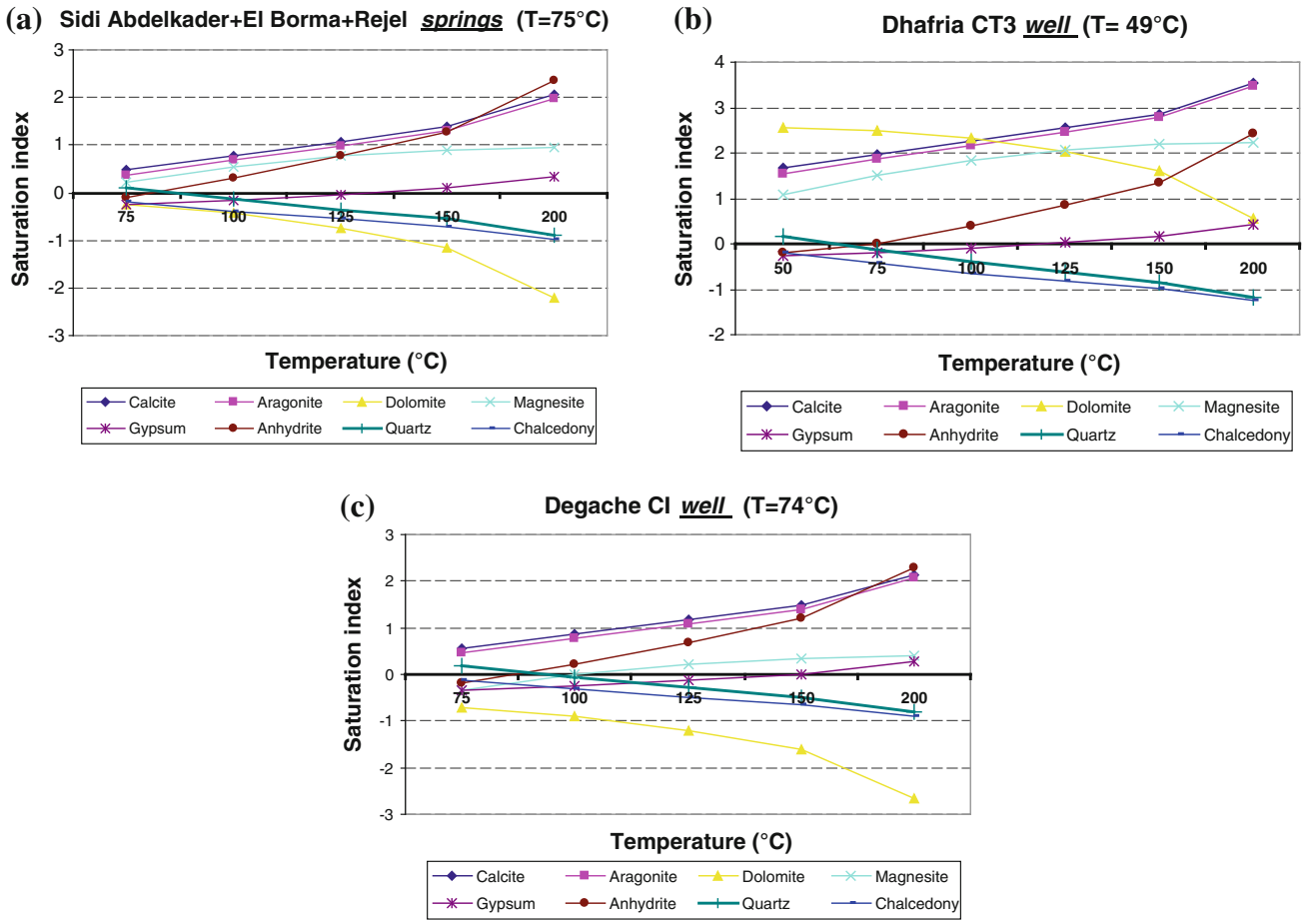

Fig. 12 Mineral equilibrium diagrams of the thermal water

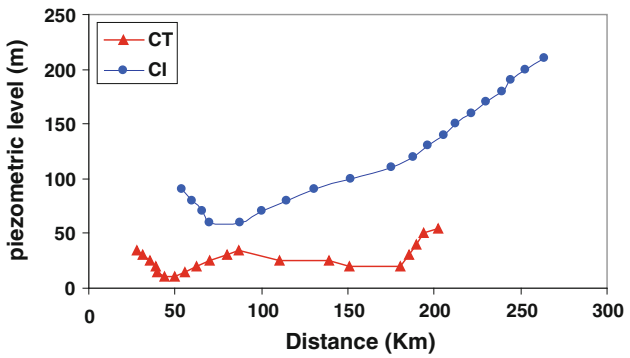

Fig. 13 Piezometric profiles of the superposed aquifers in the South-western Tunisia

Table 7 Enthalpies of liquid water, and quartz solubilities at selected temperatures [2]

Temperature (°C)	Silica (mg/l)	Enthalpy (cal/g)
50	13.5	50
75	26.6	75
100	48	100.1
125	80	125.4
150	125	151
175	185	177
200	265	203
225	365	230.9
250	486	259.2

4.5.2 Chloride Method

To further evaluate mixing in the geothermal fields, it is necessary to calculate mixing ratios. This can be achieved using hydrochemical components.

Because most waters reaching the surface are of mixed type, recognition of different components/end-members is a challenging task. This is particulary true if water–rock re-equilibration occurs after mixing (e.g if residence times are long). To simplify calculation of mixing amounts, it is assumed that the abstracted groundwater is a mixture of two end-members, one thermal and one non-thermal groundwater. Chloride is used to estimate mixing ratios, because it generally does not participate in chemical reactions even at

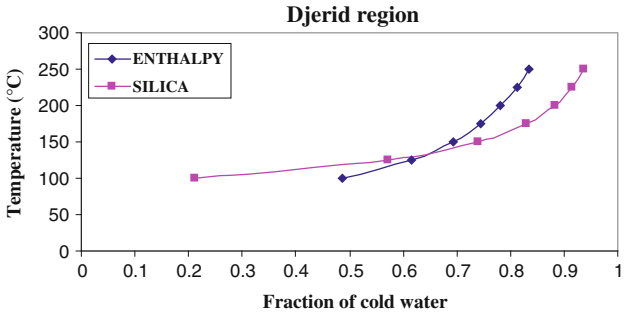

Fig. 14 Relation between fraction of cold water and temperature

high concentrations and temperatures. Assuming conservative Cl^- behavior, mixing of cold water with thermal water is estimated using the following equation [51]:

$$R = \frac{[Cl_T^-] - [Cl_{MIX}^-]}{[Cl_T^-] - [Cl_C^-]} \times 100\ (\%)$$

where R = mixing ratio, expressed as the percentage of non thermal groundwater (%); Cl_{MIX}^- = chloride concentration in the mixed groundwater; Cl_C^- = chloride concentration in the cold groundwater; Cl_T^- = chloride concentration in the thermal water.

To apply this method we have selected water samples that have different physicochemical characteristics (hot, cold and mixing) in this study area. The application of this equation shows a highest mixing ratio nearly 73 % in Tozeur region. This result is probably due to the abundant of fractures especially in the Djerid basin that promotes the ascent of thermal waters from the deep aquifer of Sidi Aïch formation (CI aquifer) to shallow zones and mixing with the water of Beglia formation of Lower Miocene CT aquifer.

4.6 Mixing Models

The evident mixing processes diminish the reliability of the subsurface temperatures estimated by solute geothermometers. In order to eliminate such mixing effects, two mixing models have been applied to evaluate the subsurface temperatures of the geothermal water in this study as outlined below.

4.6.1 Silica–Enthalpy Mixing Model

Water in many hot springs consists of mixtures of deep hot water and shallow cold water. Truesdell and Fournier [52] have proposed a plot of dissolved silica concentration versus enthalpy of water to estimate the temperature of the deep hot water component of mixed water. This model is based on the assumption that no conductive cooling has occurred after mixing. If the mixed water has cooled conductively after mixing, the calculated temperature of the hot water component

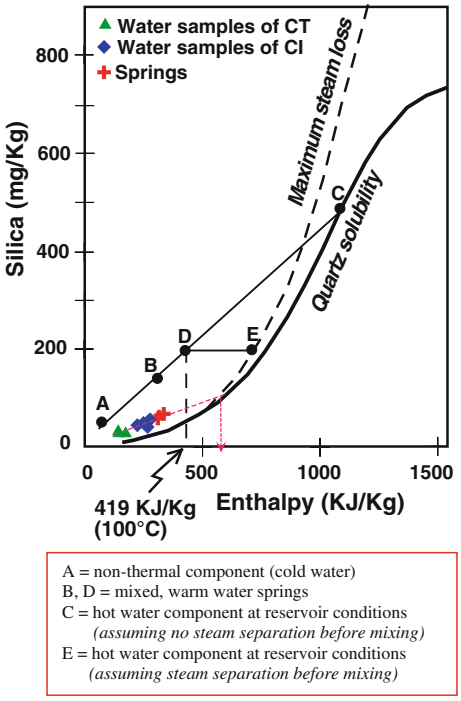

Fig. 15 Silica–enthalpy mixing model for the Djerid waters

would be too high. It is also assumed that no silica deposition takes place before or after mixing and that quartz controls the solubility of silica in hot water.

Figure 15 depicts the silica–enthalpy-mixing model applied to the Djerid water samples. For these samples, one mixing line is the result. Assuming no steam loss before mixing, this line is drawn from the cold water samples through the hot springs. The estimated enthalpy for the deep hot water is around 500 kJ/kg, which correspond to temperature of 119 °C.

The observed discrepancy between measured temperatures for the geothermal water in Djerid region and temperatures predicted by the mixing model is probably as a result of type of silica phase selected in the model. If chalcedony had been used as a controlling phase in the models instead of quartz the model results would have indicated both lower reservoir temperatures and less mixing.

4.6.2 Enthalpy–Chloride Mixing Model

Diagram plots are simple, but have proved very useful in determining models of fluid movements and hydrology by considering chloride concentration and enthalpy [53]. It is possible to use these diagrams in both exploration and development stages and they are successful for virtually all types of terrain and for both high and low temperature.

This mixing model takes into account both mixing and boiling processes. The results for the CT, CI and spring water samples from the Djerid area are shown in Fig. 16.

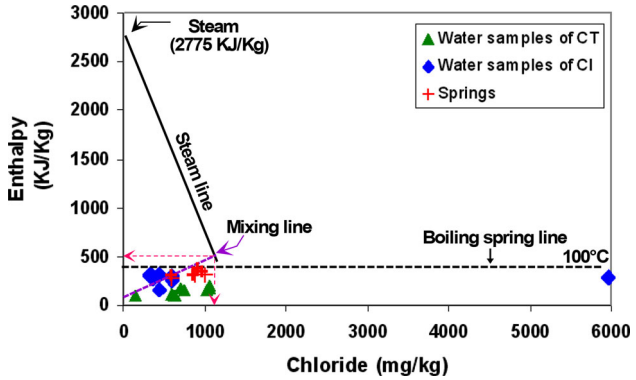

Fig. 16 Enthalpy–chloride mixing model for Djerid waters

It is clear that two types of water are observed: cold and thermal water. Thermal water of CI and spring water have been subjected to a certain degree of boiling processes, and steam loss produces loss of heat and little increase in chloride content in the liquid phase (through loss of mass, i.e. vapour). On the other hand, majority of the geothermal water have been subjected to mixing processes. Some of them plot outside the mixing zone but probably they reach the mixing zone after stabilization.

5 Conclusions

The Djerid region indicates different chemical composition of groundwaters related to different hydrogeological systems. The water of the two identified hydogeological systems is characterised by different temperatures. The CI water is classified as thermal water (temperature of about 68 °C), whereas the water of the Complex Terminal is classified as cold water (surface temperature of about 24.5 °C). Piper diagram plots reveal that waters from both the wells and springs in the Djerid region are Ca–(Na)–SO_4–(Cl) mixed water type, possibly due to the presence of evaporate minerals (gypsum and/or anhydrite ($CaSO_4$) in this two aquifers.

Individual representation (samples) in the PCA approach classifies the groundwater in two different groups: a first group representing the trend of halite dissolution essentially for CI groundwaters and a second group representing the trend of gypsum dissolution essentially for Miocene CT aquifer waters.

Using the silica geothermometers, the estimated temperature of the thermal reservoirs could be in the range of 60–104 °C, which is relatively close to the temperature estimated from equilibrium modelling (75–100 °C).

The water temperatures vary considerably suggesting mixing of ascending thermal water with shallow cold water. The contribution of cold water in mixing is estimated from the enthalpy and chloride methods to be about 65 and 73 % respectively. A plot of dissolved silica vs. enthalpy of the liquid water gives a maximum temperature of 119 °C for the hot water component. Similarly the enthalpy chloride mixing model yields a reservoir temperature of about 105 °C.

Acknowledgments The authors warmly thank the anonymous reviewers for their detailed and constructive comments, which were of great help in improving this manuscript.

References

1. Truesdell, A.H.: Summary of section III-geochemical techniques in geothermal exploration. In: Proceedings, Second U.N. Symposium on the Development and Use of Geothermal Resources, San Francisco, vol. 1, pp. 1iii–1xiii (1975)
2. Fournier, R.O.; Truesdell, A.H.: Geochemical indicators of subsurface temperature-part 2, estimation of temperature and fraction of hot water mixed with cold water. J. Res. U.S. Geol. Surv. **2**, 263–270 (1974)
3. Arnorsson, S.: Chemical equilibria in Icelandic geothermal systems-implications for chemical geothermometry in investigations. Geothermics **12**, 119–128 (1983)
4. Reed, M.; Spycher, N.: Calculation of pH and mineral equilibria in hydrothermal waters with application to geothermometry and studies of boiling and dilution. Geochim. Cosmochim. Acta **48**, 1479–1492 (1984)
5. Mahon, W.A.J.: Chemistry in the exploration and exploitation of hydrothermal systems. In: Proceedings United Nations Symposium on the Development-and Utilization of Geothermal Energy: Pisa, vol. 2, Part 2, Geothermics, Spec. Issue 2, pp. 1310–1322 (1970)
6. Tonani, F.: Geochemical methods of exploration for geothermal energy. In: Proceedings U.N. Symposium on the Development and Utilization of Geothermal Resources, Pisa, 1970, vol. 2, Part 1. Geothermics, Spec. Issue 2, pp. 492–515 (1970)
7. White, D.E.: Geochemistry applied to the discovery, evaluation and exploitation of geothermal energy resource. In: Proceedings United Nations Symposium on the Development and Utilization of Geothermal Energy: Pisa, vol. 1, Part 2, Geothermics, Spec. Issue 2, pp. 58–80 (1970)
8. Fournier, R.O.; Truesdell, A.H.: An empirical Na–K–Ca geothermometer for natural waters. Geochim. Cosmochim. Acta **37**, 1255–1275 (1973)
9. Ellis, A.J.; Mahon, W.A.J.: Chemistry and Geothermal Systems. Academic Press, New York (1977)
10. Fournier, R.O.; Potter, R.W., II.: Magnesium correction to Na–K–Ca geothermometer. Geochim. Cosmochim. Acta **43**, 1543–1550 (1979)
11. Giggenbach, W.F.; Gonfiantini, R.; Jangi, B.L.; Truesdell, A.H.: Isotopic and chemical composition of Parbati valley geothermal discharges, NW-Himalaya, India. Geothermics **12**, 199–222 (1983)
12. Giggenbach, W.F.: Geothermal solute equilibria. Derivation of Na–K–Mg–Ca geoindicators. Geochim. Cosmochim. Acta **52**, 2749–2765 (1988)
13. Pauwels, H.; Fouillac, C.; Fouillac, A.M.: Chemistry and isotopes of deep geothermal saline fluids in the Upper Rhine Graben: origin of compounds and water–rock interactions. Geochim. Cosmochim. Acta **51**. 2737–2749 (1993)
14. Tarcan, G.; Gemici, Ü.: Water geochemistry of the Seferihisar geothermal area, Izmir, Turkey. J Volcanol. Geotherm. Res. **126**, 225–242 (2003)
15. Ben Dhia, H.: Geothermal energy in Tunisia: potential of the southern province. Geothermics **16**, 299–318 (1987)

16. Ben Brahim, F.; Makni, J.; Bouri, S.; Ben Dhia, H.: Properties of geothermal resources in Kebilli region, Southwestern Tunisia. J. Environ. Earth Sci. (2012). doi:10.1007/s12665-012-1974-7
17. Ben Brahim, F.: Caractérisation hydrogéologique, hydrochimique et géothermique des systèmes aquifères du Sud ouest Tunisien. Thèse Doctorat en Sciences géologiques. Faculté des Sciences de Sfax- Tunisie (2013)
18. Zouaghi, T.; Guellala, R.; Lazzez, M.; Bedir, M.; Ben Youssef, M.; Inoubli, M.H.; Zargouni, F.: The Chotts fold belt of Southern Tunisia, North African margin: structural pattern, evolution, and regional geodynamic implications. In: Schattner, U. (Ed.) New Frontiers in Tectonic Research—At the Midst of Plate Convergence. ISBN: 978-953-307-594-5 (2011)
19. Zargouni, F.; Rabia. M.C.H.; Abbes, C.: Rôle des couloirs de cisaillement de Gafsa et de Negrine-Tozeur dans la structuration du Faisceau Sud-atlasique. C.R. Acad. Sc. Paris. T-301, série II, pp. 831–834 (1985)
20. Ben Ayed, N.: Evolution tectonique de l'avant-pays de la chaine alpine de Tunisie du début du Mésozoïque à l'Actuel. Annales des Mines et de la Géologie de Tunisie, n°32. Tunisie (1993)
21. Zouari, H.: Evolution géodynamique de l'Atlas centro-méridional de la Tunisie. Stratigraphie, analyses géométrique, cinématique et tectono-sédimentaire. Thèse Doct. es-Sciences, Univ. Tunis II (1995)
22. Bouaziz, S.: Etude de la tectonique cassante dans la plateforme et l'Atlas Sahariens (Tunisie Méridionale): Evolution des paléochamps de contraintes et implications géodynamiques. Thèse de Doctorat, Fac. Sc. De Tunis (1995)
23. Bédir, M.: Mécanismes géodynamiques des bassins associés aux couloirs de coulissements de la marge atlasique de la Tunisie. Seismo-stratigraphie, seismotectonique et implications pétrolières. Thèse Doct. es Sciences, Univ. Tunis II. Tunisie (1995)
24. Hlaiem, A.: Halokinesis and structural evolution of the major features in eastern and southern Tunisian Atlas. Tectonophysics **306**(1), 79–95 (1999)
25. Zouaghi, T.; Bédir, M.; Inoubli, M.H.: Structuration profonde des dépôts de l'Albien-Maastrichtien en Tunisie centrale: nouvelle limite de l'archipel de Kasserine et implications géodynamiques. Comptes Rendus Geoscience **337**, 685–693 (2005)
26. Lazzez, M.; Zouaghi, T.; Ben Youssef, M.: Austrian phase on the northern African margin inferred from sequence stratigraphy and sedimentary records in southern Tunisia (Chotts and Djeffara areas). Comptes Rendus Geoscience **340**, 543–552 (2008)
27. Mannai-Tayech, B.; Otera, O.: Un nouveau gisement miocène à ichthyofaune au Sud de la chaine des Chotts (Tunisie méridionale). C.R. Palevol. **4**, 405–412 (2005)
28. Mannai-Tayech, B.: The lithostratigraphy of Miocene series from Tunisia, revisited. J. Afr. Earth Sci. **54**, 53–61 (2009)
29. Swezey, C.: Cenozoic stratigraphy of the sahara, northern Africa. J. Afr. Earth Sci. **53**, 89–121 (2009)
30. Cornet, A.: Introduction à l'hydrogéologie saharienne. Revue de Géographie Physique et Géologie Dynamique, pp. 5–72 (1964)
31. Castany, G.: Bassin sédimentaire du Sahara septentrional (Algérie-Tunisie). Aquifères du Continental Intercalaire et du Complexe Terminal, Bull. Bur. Rec. Géol. Min. (BRGM), Sér. **2, 3**, 127–147 (1982)
32. Edmunds, W.M.; Guendous, A.H.; Mamou, A.; Moula, A.; Shand, P.; Zouari, K.: Groundwater evolution in the continental intercalary aquifer of Southern Algeria and Tunisia: trace element and isotopic indicators. Appl. Geochem. **18**, 805–822 (2003)
33. Mamou, A.: Caractérisation et évaluation des ressources en eau du Sud tunisien. Thèse de doctorat d'état en sciences naturelles. Univ. Paris-Sud, centre d'Orsay, p. 403 (1990)
34. Piper, A.M.: A graphic procedure in the geochemical interpretation of water analyses. Trans. Am. Geophys. Union **25**, 914–923 (1944)
35. Nair, R.; Kalariya, T.; Sumitra, C.: Antibacterial activity of some selected Indian medicinal flora. Turk. J. Biol. **29**, 41–47 (2005)
36. Nicholson, K.: Geothermal Fluids; Chemistry and Exploration Techniques. Springer, Berlin (1993)
37. Rybach, L.; Muffler, L.J.P.: Geothermal Systems: Principles and Case Histories. Wiley, UK, p. 34 (1981)
38. Kharaka, Y.K.; Mariner, R.H.: Chemical geothermometers and their applications to waters from sedimentary basins. In: Thermal History of Sedimentary Basins, S.C.P.M. Special Volume, pp. 99–117 (1989)
39. Fournier, R.O.: Chemical geothermometers and mixing models for geothermal systems. Geothermics **5**(1/4), 41–50 (1977)
40. D'Amore, F.; Fancelli, R.; Caboit, R.: Observations on the application of chemical geothermometers to some hydrothermal system in Sardinia. Geothermics **16**, 271–282 (1987)
41. Lopez-Chicano, M.; Bouamama, M.; Vallejeos, A.; Publido, B.A.: Factors which determine the hydrogeochemical behavior of karst springs. A case study from the Betic Cordilleras, Spain. Appl. Geochem. **16**, 1179–1192 (2001)
42. Mark, C.P.: Hydrogeochemistry and geothermometry of thermal groundwaters from the Birdsville Track Ridge, Great Artesian Basin, South Australia. Geothermics **33**, 743–774 (2004)
43. Crerar, A.D.: A method for computing multicomponent chemical equilibria based equilibrium constants. Geochim. Cosmochim. Acta **39**, 1375–1384 (1975)
44. D'Amore, F.; Fancelli, R.; Caboit, R.: Observations on the application of chemical geothermometers to some hydrothermal system in Sardinia. Geothermics **16**, 271–282 (1987)
45. D'Amore, F.; Mejía, J.T.: Chemical and physical reservoir parameters at initial conditions in Berlin geothermal field El Salvador: a first assessment. Geothermics **28**, 45–73 (1999)
46. Tole, M.P.; Armannsson, H.; Pang, Z.; Arnorsson, S.: Fluid/mineral equilibrium calculations for geothermal fluids and chemical geothermometry. Geothermics **22**, 17–37 (1993)
47. Pang, Z.; Reed, M.H.: Theoretical chemical geothermometry on geothermal waters: problems and methods. Geochim. Cosmochim. Acta **62**, 1083–1091 (1998)
48. Taran, Y.A.; Rouwet, D.; Inguaggiato, S.; Aiuppa, A.: Major and trace element geochemistry of neutral and acidic thermal springs at El Chichón volcano, Mexico: implications for monitoring of the volcanic activity. J. Volcanol. Geotherm. Res. **178**, 224–236 (2008)
49. Calmbach, L.: HYDROWIN: computer programme, version 3.0. Institut de Minéralogie BFSH 2, 1015. Uni-Lausanne, Switzerland (1995)
50. Gupta, H.; Roy, S.: Geothermal Energy: An Alternative Resource for the 21st Century. Elsevier, Amsterdam, p. 279 (2007)
51. Han, D.M.; Liang, X.; Jin, M.G.; Currell, M.J.; Song, X.F.; Liu, C.M.: Evaluation of groundwater hydrochemical characteristics and mixing behaviour in the Daying and Qicun geothermal systems, Xinzhou Basin (2010)
52. Truesdell, A.H.; Fournier, R.O.: Procedure of estimating the temperature of a hot-water component in a mixed water by using a plot of silica versus enthalpy. J. Res. U.S. Geol. Surv. **5**, 49–52 (1977)
53. Fournier, R.O.: Application of water geochemistry to geothermal exploration and reservoir engineering. In: Rybach, L.; Muffler L.J.P. (eds.) Geothermal Systems: Principles and Case Histories. Wiley and Sons, New York, pp. 109–143 (1981)